연구논문집 제5권 제1호p. 5~12 1974

Momentum Distributions and Compton Profiles of CH_2 Molecule*

Nha, Sang Kyun and Cho, Hwa Shuk
Dept. of Materials Science
and Engineering

〈**Abstract**〉

Momentum distributions and Compon profiles are calculated for CH_2 molecule by transforming (1) free atom, (2) self-consistent field, and (3) localized molecular orbital wavefunctions from position space to momentum space. The comparison of the Compton profiles with available experimental one has shown that the wavefunctions of (1) and (3) are definitely better than those of (2) for describing the motion of electrons in CH_2 molecule. It is suggested that the localized molecular orbital wavefunctions can be used for predicting the distributions and profiles of several homologous series of organic molecules for which accurate wavefunction calculations are unfeasible.

CH_2 分子의 運動量分布와 Compton Profile

羅 商 均·趙 和 錫
材料工學科

〈요 약〉

(1) 自由原子, (2) self-consistent場, 및 (3) 局所分子軌道의 波動函數를 位置空間에서 運動量空間으로 變換시켜 CH_2分子의 運動量 分布와 Compton profile을 計算하였다. 實驗値와 比較하므로서 (1)과 (3)의 波動函數가 (2)의 것보다 더 正確하게 CH_2 分子 內의 電子運動을 記述함을 알게 되었다. 局所分子軌道 波動函數를 利用하여 分子波動函數가 알려지지 않는 CH_2와 類似構造의 有機分子들의 運動量과 Compton profile을 豫測할 수 있다고 본다.

1. Introduction

The calculation of the momentum distributions and the Compton profiles has been of interest to theoretical chemists and physicists. Since the momentum distribution of the electrons determines the shape of the Compton profile, and the momentum distribution is directly related to the motion of electrons, knowledge about the electron motion can be obtained through the study of these momentum distributions and the Compton profiles. The calculation has met, however, with two major obstacles. First, the lack of good position space wavefunctions has hindered the application of methods which use these functions as a starting point. In addition, a scarcity of experimetal results, particularly for molecules, has made comparison of theory with experiment difficult.

Recent advances in theoretical and experimental techniques have made possible both the

*Supported by the Ministry of Education, Republic of Korea.

calculation of vastly improved position space wavefunctions and the accurate measurement of Compton profiles. One[1] of the present authors has developed very recently the theory of the Doppler broadening (or Compton profile) of the electromagnetic waves scattered by the Compton process on the moving electrons. He has also measured the Compton profiles of three atoms and one molecule and has shown that the motion of electrons can be studied by the investigation of the shape of the Compton profiles.

The molecular momentum distributions and the Compton profiles were the subject of a pioneering series of papers by Coulson and Duncanson[2] and many other workers.[3] In this paper, calculations have been carried out for CH_2 molecule by making use of the position space wavefunctions given by three different approximations of (1) free atom (FA), (2) self-consistent field (SCF), and (3) localized molecular orbital (LMO).

The purpose of this work is thus to present the results of the CH_2 molecular momentum distributions and the Compton profiles to investigate the sensitivity of the approximations to the motion of electrons in CH_2 molecule. Because of the idea that similar orbitals make similar contributions to the Compton profile, the possibility of using our method to study the electron motion of related molecules is also briefly discussed.

II. Molecular Momentum Distributions

The momentum wavefunction of an atomic or molecular system is obtained from its position space wavefunction by means of the Dirac transformation theory:

$$F(\vec{P})=\frac{1}{(2\pi\hbar)^{3/2}}\int e^{-\frac{i}{\hbar}\vec{P}\cdot\vec{r}}\phi(\vec{r})d\vec{r} \qquad (2.1)$$

This transformation has the useful property that it preserves the form of the wavefunction and is independent of the spin functions. The square of the absolute value of the momentum wavefunctions, $|F(\vec{P})|^2$, gives the density in momentum or the probability of encountering an electron. The momentum distribution can be calculated at once from the momentum wavefunction. Thus, if there is only one electron,

$$W(P)=\int|F(\vec{P})|^2\vec{P}^2d\Omega, \qquad (2.2)$$

where $d\Omega$ is an element of solid angle for electron momentum.

We must therefore decide what form we shall take for the position space wavefunction $\phi(\vec{r})$ to use Eq. (2.1). Except for the hydrogen atom, however, the positon space wavefunction for complex atom and molecule cannot be solved exactly because of the complicated form of the potential energy in Hamiltonian. Thus, all methods used for obtaining position space wavefunctions are approximate.

1. Free Atom Approximation

The CH_2 molecular wavefunction is assumed to be described by the free atomic wavefunctions for H and C. The electron population of CH_2 is, then, two 1s electrons in H, and two 1s, two 2s, and two 2p electrons in C. Let $\phi_{lmn}(\vec{r})$ be an electronic wavefunction characterized by the quantum numbers l, m, and n, where l is the principal quantum number, m the azimuthal quantum number, and n the magnetic quantum number, then $\phi_{lmn}(\vec{r})$ can be expressed as products of radial wavefunction $a_{lm}(r)$ and angular wavefunction or spherical harmonics $Y^n{}_m(\theta,\varphi)$:

$$\phi_{lmn}(\vec{r})=a_{lm}(r)Y^n{}_m(\theta,\varphi). \qquad (2.3)$$

For the calculation of the momentum wavefunction, we denote the angle between $\vec{r}(r,\theta,\varphi)$ and $\vec{P}(P,\Theta,\Phi)$ by α, and introduce $\vec{k}=\frac{\vec{P}}{\hbar}$. The expansion of the exponential term in Eq. (2.1) is then given by

$$e^{-ikr\cos\alpha}=\sum_{J=0}^{\infty}(2J+1)(-1)^J\left(\frac{\pi}{2kr}\right)^{\frac{1}{2}}\times J_{J+\frac{1}{2}}(kr)\ P_J(\cos\alpha), \qquad (2.4)$$

where $J_{J+\frac{1}{2}}$ is a Bessel function of the first kind of the order of $J+\frac{1}{2}$ and P_J is a Legendre

polynomial of order j. The addition theorem for $P_j(\cos\alpha)$ gives, also,

$$P_j(\cos\alpha)=\frac{4\pi}{2j+1}\sum_{m'=-j}^{j}Y_j^{m'}(\Theta,\Phi)\,Y_j^{*m'}(\theta,\varphi), \tag{2.5}$$

where $\alpha=\Theta-\theta$.

Substituting Eqs. (2.3), (2.4), and (2.5) into Eq. (2.1), the expression for the momentum wavefunction $F_{lmn}(\vec{k})$ becomes

$$\begin{aligned}F_{lmn}(\vec{k})=&\frac{1}{(2\pi\hbar)^{3/2}}\int_0^\infty r^2dr\int_{-1}^{1}d(\cos\theta)\\&\times\int_0^{2\pi}d\phi a_{lm}(r)Y^n{}_m(\theta,\varphi)\\&\times\sum_{j=0}^{\infty}(2j+1)(-1)^j\left(\frac{\pi}{2kr}\right)^{\frac{1}{2}}\\&\times J_{j+\frac{1}{2}}(kr)\frac{4\pi}{2j+1}\\&\times\sum_{m'=-j}^{j}Y_j^{m'}(\Theta,\Phi)Y_j^{*m'}(\theta,\varphi).\end{aligned} \tag{2.6}$$

Integrating over the angles and using the orthogonal properties of $Y^n{}_m$ functions, the expression for $F_{lmn}(k,\Theta,\Phi)$ becomes

$$\begin{aligned}F_{lmn}(k,\Theta,\Phi)=&\left(\frac{2}{\pi}\right)^{1/2}\int_0^\infty r^2dr(-i)^m\\&a_{lm}(r)j_m(kr)Y^n{}_m(\Theta,\Phi),\end{aligned} \tag{2.7}$$

where the spherical Bessel functions $j_j(\rho)=\left(\frac{\pi}{2\rho}\right)^{1/2}J_{j+\frac{1}{2}}(\rho)$ has been introduced.

Since the scattering atoms are oriented in random fashion, the quantity required is the momentum distribution, $W_{lm}(P)$, of the electron having a momentum lying between P and $P+dP$ when the atoms averaged over all angles, Θ and Φ. This quantity is simply the average of $|F_{lmn}(P)|^2$ over all angles multiplied by P^2:

$$\begin{aligned}W_{lm}(P)=&\frac{1}{4\pi}\int_{-1}^{1}d(\cos\Theta)\\&\times\int_0^{2\pi}d\Phi P^2|F_{lmn}(P,\Theta,\Phi)|.\end{aligned} \tag{2.8}$$

For all of the electrons in atom, the momentum distribution is then

$$W(P)=\sum_l\sum_m W_{lm}(P) \tag{2.9}$$

For CH_2 molecule, it is just a superposition of the momentum distributions of H and C:

$$W_{CH_2}=W_H+W_C. \tag{2.10}$$

The Calculation of W_{CH_2} is carried out in the methods described above by using the Herman and Skillman free atom radial wavefunctions[4] for H and C and results are shown in Fig. 1.

2. Self-Consistent Field Approximation

Using the approximate Hartree-Fock molecular orbitals and employing self-consistent field (SCF) method, Krauss[5] has recently calculated the CH_2 molecular wavefunctions. With molecule aligned along the z-axis, the molecular orbitals for CH_2 are considered to be

$$(1\sigma_g)^2(2\sigma_g)^2(1\sigma_u)^2(\pi_x)^1(\pi_y)^1,$$

where two electons are put in all states of σ orbits except for π orbits which are each singly occupied.

The molecular SCF wavefunctions for CH_2 can be written in the following forms:

$$\begin{aligned}\phi_{1\sigma_g}(r)&=\sum_{i=1}^{9}A_ie^{-a_ir^2}+\frac{1}{2}\sum_{i=1}^{3}M_i(e^{-m_ir_1^2}+e^{-m_ir_2^2})\\\phi_{2\sigma_g}(r)&=\sum_{i=1}^{9}B_ie^{-a_ir^2}+\frac{1}{2}\sum_{i=1}^{3}N_i(e^{-m_ir_1^2}+e^{-m_ir_2^2})\\\phi_{1\sigma_u}(r)&=\sum_{i=1}^{5}C_ize^{-b_ir^2}+\frac{1}{2}\sum_{i=1}^{3}O_i(e^{-m_ir_1^2}+e^{-m_ir_2^2})\\\phi_{\pi_x}(r)&=\sum_{i=1}^{6}D_ixe^{-b_ir^2}\end{aligned} \tag{2.11}$$

and $\phi_{\pi_y}(r)=\sum_{i=1}^{6}D_iye^{-b_ir^2}$.

Here, r_1 and r_2 are the distance of the electron from the first and the second H atom, respectively, and $d=1.35$ bohr radii spacing, and r is the distance from C to electron such that $\vec{r}_1+\vec{d}=\vec{r}$ and $\vec{r}=\vec{r}_2-\vec{d}$. A, B, C, D, M, N, and O are the eigenvector coefficients, and a, b, and m are the parameters for the basis orbitals.

The momentum distributions of CH_2 molecule can now be calculated by transforming the SCF wavefunctions from position space to momentum space. Resolving $\vec{k}$ and $\vec{r}$ vectors into their cartesian coordinate, we have $\vec{k}\cdot\vec{r}=k_xx+k_yy+k_zz$ and $e^{-ar^2}=e^{-ax^2}e^{-ay^2}e^{-az^2}$. Since the integral of a sum is the sum of the integrals, the transformation gives the momentum wavefunctions. They are

$$\begin{aligned}F_{1\sigma_g}(k)=&\sum_{i=1}^{9}A_i\left(\frac{\pi}{a_i}\right)^{3/2}e^{-\frac{k^2}{4a_i}}\\&+\sum_{i=1}^{3}M_i\left(\frac{\pi}{m_i}\right)^{3/2}e^{-\frac{k^2}{4m_i}}\cos(\vec{k}\cdot\vec{d}),\end{aligned}$$

$$F_{2\sigma_g}(k)=\sum_{i=1}^{9}B_i\left(\frac{\pi}{a_i}\right)^{3/2}e^{-\frac{k^2}{4a_i}}+\sum_{i=1}^{3}N_i\left(\frac{\pi}{m_i}\right)^{3/2}e^{-\frac{k^2}{4m_i}}\cos(\vec{k}\cdot\vec{d}),$$

$$F_{1\sigma_u}(k)=i\sum_{i=1}^{5}\frac{1}{2}C_i\left(\frac{\pi}{b_i}\right)^{3/2}\left(\frac{k_z}{b_i}\right)e^{-\frac{k^2}{4b_i}}+i\sum_{i=1}^{3}O_i\left(\frac{\pi}{m_i}\right)^{3/2}e^{-\frac{k^2}{4m_i}}\sin(\vec{k}\cdot\vec{d})$$

$$F_{\pi_y}(k)=i\sum_{i=1}^{5}\frac{1}{2}D_i\left(\frac{\pi}{b_i}\right)^{3/2}\left(\frac{k_x}{b_i}\right)e^{-\frac{k^2}{4b_i}},$$

and

$$F_{\pi_y}(k)=i\sum_{i=1}^{5}\frac{1}{2}D_i\left(\frac{\pi}{b_i}\right)^{3/2}\left(\frac{k_y}{b_i}\right)e^{-\frac{k^2}{4b_i}}. \quad (2.12)$$

We omit the details of the calculations of the momentum distributions, but it follows from Eq. (2.2) that the explicit expression for the momentum distribution for the $1\sigma_g$ orbit electron is

$$W_{1\sigma_g}(k)=\pi^3k^2\Big[\sum_{i=1}^{9}\frac{A_i^2}{a_i^3}e^{-\frac{k^2}{2a_i}}+\frac{1}{2}\sum_{i=1}^{3}\frac{M_i^2}{m_i^3}e^{-\frac{k^2}{2m_i}}\left(1+\frac{1}{2}\frac{\sin(2kd)}{kd}\right)+2\sum_{i\neq j}^{9}\frac{A_iA_j}{(a_ia_j)^{3/2}}e^{-\frac{k^2}{4}\left(\frac{1}{a_i}+\frac{1}{a_j}\right)}+\sum_{i\neq j}^{3}\frac{M_iM_j}{(m_im_j)^{\frac{3}{2}}}e^{-\frac{k^2}{4}\left(\frac{1}{m_i}+\frac{1}{m_j}\right)}\times\left(1+\frac{1}{2}\frac{\sin(2kd)}{kd}\right)+2\sum_{i,j}^{9}\frac{A_iM_i}{(a_im_i)^{3/2}}e^{-\frac{k^2}{4}\left(\frac{1}{a_i}+\frac{1}{m_j}\right)}\times\frac{\sin(kd)}{kd}\Big]. \quad (2.13)$$

The $2\sigma_g$ orbit electron momementum distribution will have the same form as $1\sigma_g$ with the eigenvector coefficients B and N instead of A and M in Eq. (2.13). Similarly, the momentum distribution for $1\sigma_u$ orbital electron becomes

$$W_{1\sigma_u}(k)=\pi^3k^2\Big[\frac{k^2}{12}\sum_{i=1}^{5}\frac{C_i^2}{b_i^5}e^{-\frac{k^2}{2b_i}}+\frac{k^2}{12}\sum_{i\neq j}^{5}\frac{C_iC_j}{(b_ib_j)^{5/2}}e^{-\frac{k^2}{4}\left(\frac{1}{b_i}+\frac{1}{b_j}\right)}+\frac{1}{2}\sum_{i=1}^{3}\frac{O_i^2}{m_i^3}e^{-\frac{k^2}{2m_i}}\left(1-\frac{1}{2}\frac{\sin(2kd)}{kd}\right)+\frac{1}{2}\sum_{i\neq j}^{3}\frac{O_iO_j}{(m_im_j)^{3/2}}e^{-\frac{k^2}{4}\left(\frac{1}{m_i}+\frac{1}{m_j}\right)}\times\left(1-\frac{1}{2}\frac{\sin(2kd)}{kd}\right)+\frac{1}{2}\sum_{i,j}^{5}\frac{C_iO_i}{b_i(b_im_j)^{3/2}}e^{-\frac{k^2}{4}\left(\frac{1}{b_i}+\frac{1}{m_j}\right)}\times\frac{1}{kd^2}\left(\sin(kd)-(kd)\cos(kd)\right)\Big]. \quad (2.14)$$

The π orbital momentum distributions, $W_{\pi_x}(k)$ $=W_{\pi_y}(k)$, are

$$W_\pi=\frac{\pi^3k^4}{6}\Big[\sum_{i=1}^{5}\frac{D_i^2}{b_i^5}e^{-\frac{k^2}{2b_i}}+\sum_{i\neq j}^{5}\frac{A_iA_j}{(b_ib_j)^{5/2}}e^{-\frac{k^2}{4}\left(\frac{1}{b_i}+\frac{1}{b_j}\right)}\Big]. \quad (2.15)$$

The close analytical expressions for the momentum distributions are thus obtained for the approximate Hartree-Fock orbital electrons in CH_2. The total momentum distribution of CH_2 molecule is then simply the sum of a suitable number of separate functions $W_{1\sigma_g}$, $W_{2\sigma_g}$, $W_{1\sigma_u}$, and W_π. Thus, we have

$$W_{CH_2}=2W_{1\sigma_g}+2W_{2\sigma_g}+2W_{1\sigma_u}+1W_{\pi_x}+1W_{\pi_y} \quad (2.16)$$

and results of calculations are given in Fig. 1.

3. Localized Molecular Orbital Approximation

The physical significance of the orbitals resulting from the SCF calculations is less clear. The orbitals of molecule can be easily interpretable in terms of chemical notions such as bonds or inner shells.

By carrying out a unitary transformation which maximizes the self-repulsion energy of the orbitals one may obtain a new set of orbitals which leave the total wavefunction unchanged, but which correspond to the concepts of bonds, inner shells and lone pairs. Since these "chemical orbitals" are of great importance in the molecular system and since it is desirable to maintain a physically interpretable picture, if possible, a study of the role of these localized molecular orbitals (LMO) in momentum space is here considered.

Considering CH_2 as a $-CH_2-$ group of C_nH_{2n+2}, $-CH_2-$ generates three categories of localized orbitals: carbon inner shells, carbon-hydrogen bonds, and carbon-carbon bonds. The radial momentum distribution of CH_2 is then given as a sum of contributions from thos e carbon inner shells, C-H bonds, and C-C bond:

$$W_{CH_2}=W_{1sC}+2W_{C-H}+W_{C-C}. \quad (2.17)$$

This follows from the fact that each unit in CH_2 has one carbon with its 1s electron (1s C), two C-H bonds, and one C-C bond. Epstein's data[6] were here used for the calculation of the LMO momentum distribution for $-CH_2-$ group. The results are shown in Fig. 1.

III. Compton Profiles

Nha's[1] analysis was summarized in the following. It is well known that the electromagnetic waves scattered by electrons at rest show an incrase in wavelength so called the Compton line:

$$\lambda_c=\lambda_1+\lambda_e(1-\cos\theta), \qquad (3.1)$$

where θ is the angle of scattering and λ_e electron Compton wavelength. Electrons in atoms and molecules are, of course, not at rest. They posses a velocity or momentum distibution determined by the momentum wevefunction, which can be calculated by the methods described in Section II. Because of the electron motion during the scattering process, the Compton line is broadened. The broadening (other than experimental) of the Compton line, which is called the Compton profile, thus, depends on the incident wavelength λ_1, the angle of scattering θ, and the electron velocity. For the fixed λ_1 and θ, the Compton profile is only related to the motion of electrons. $\lambda_1=9.35\times10^{-3}$Å and $\theta=60°$ are used for this calculation.

Because of the line broadening due to the electron motion there exist a shift in wavelength, l, of the scattered electromagnetic wave from its value λ_c. It was shown that this shift can be expressed as

$$l=\lambda_2-\lambda_c=2\beta\lambda^*\cos\phi/(1-\beta\cos\theta_1). \qquad (3.2)$$

Here, λ_2 is the wavelength of the electromagnetic waves scattered through the moving electron, θ_1 is the angle between the initial electron momentum and the initial electromagnetic wave momentum, ϕ is the angle between the initial electron momentum and a new reference axis which lies in the direction of the change in momentum of the electromagnetic wave for the scattering from a stationary electron, while λ^* is defined by

$$2\lambda^*=(\lambda_c^2+\lambda^2{}_1-2\lambda_c\lambda_1\cos\theta)^{1/2}. \qquad (3.3)$$

The relation between θ_1 and ϕ is given by

$$\cos\theta_1=\sin\phi\cos\chi\sin\gamma+\cos\phi\cos\gamma, \qquad (3.4)$$

where χ is the azimuthal angle of the initial electron momentum measured from the scattering plane and

$$\cos\gamma=\frac{4\lambda^{*2}+\lambda_c{}^2-\lambda_1{}^2}{4\lambda_c\lambda^*}. \qquad (3.5)$$

The relation between the electron velocity and the wavelength shift in the scattering process is given in Eq. (3.2). The relation between the Compton profile, $P(l)$, and the momentum distribution, $W(\beta)$, is, thus, given by Eq. (3.2). The distribution of electronic momentum, therefore, give rise to a shape of Compton profile:

$$P(l)=\int_{\beta_{\min}}^{1}\frac{W(\beta)(1-\beta^2\cos\gamma)}{4\beta\lambda^*}d\beta. \qquad (3.6)$$

A scattering experiment might measure the energy spectrum, $P(\epsilon)$, rather than the wavelength spectrum, $P(l)$. Here, $\epsilon=E(\beta)-E_c$ is the shift in the energy of the scattered electromagnetic waves and $E_c=E(\beta=0)$ the energy of the λ_c. Now $E=\frac{hc}{\lambda}$, so that $dE=-\frac{E}{\lambda}d\lambda$, or

$$\epsilon=-\frac{E_c}{\lambda_c}l \qquad (3.7)$$

for $\epsilon\ll E_c$. Since, by definition $P(\epsilon)d\epsilon=P(l)dl$, the Compton profile in the energy coordinate can be written in terms of the electron momentum distribution:

$$P(\epsilon)=\frac{\lambda_c}{E_c}\int_{\beta_{\min}}^{1}\frac{W(\beta)(1-\beta^2\cos\gamma)}{4\beta\lambda^*}d\beta. \qquad (3.8)$$

The calculations were performed, then, as follows. The position space wavefunctions were used to find $W(\beta)$ as outlined in Section II. The energy spectrum of the Compton profile, $P(\epsilon)$, was, then, obtained from $W(\beta)$ as just described.

IV. Results and Discussion

Fig. 1 shows the CH_2 molecular momentum distributions calculated on the basis of (1) FA.

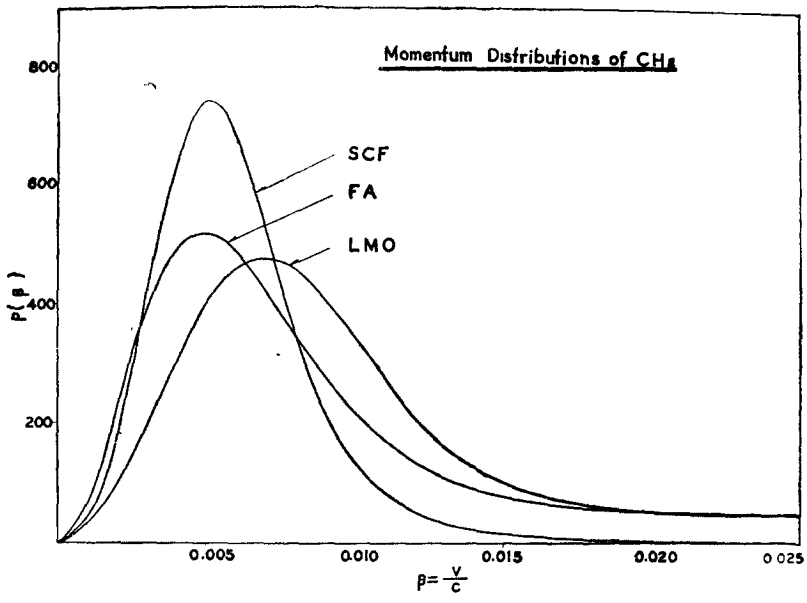

Fig. 1 Momentum distributions of CH_2 molecule calculated by transforming (1) free atom (FA), (2) self-consistent field (SCF), and localized molecular orbital (LMO) wavefunctions from position space to momentum space.

(2) SCF, and (3) LMO approximations. Distributions were normalized by equalizing the area under the distribution curves. As seen in Fig. 1, a large discrepancy among those three distributions was found not only in height, but also particularly in the relative importance of the tail at the high momentum region. The FA and SCF momentum distributions reach their maxi-

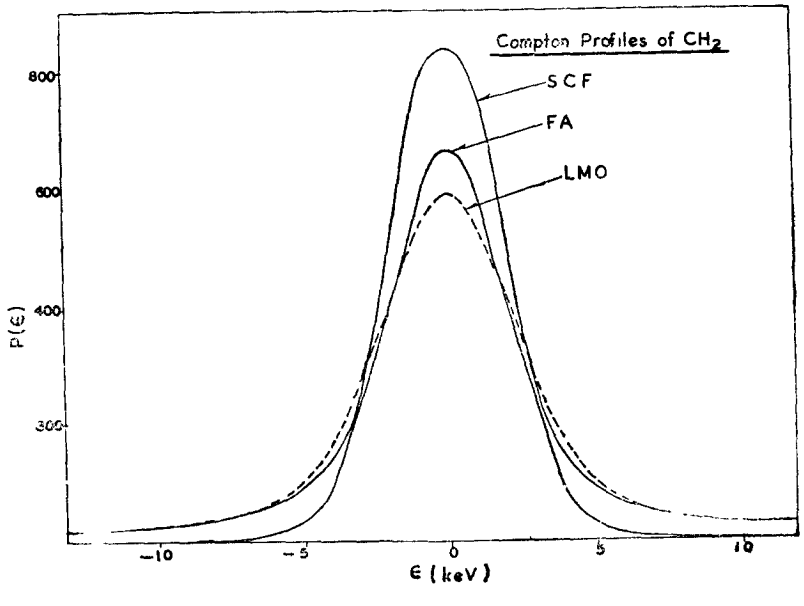

Fig. 2 Compton profiles of CH_2 molecule obtained from (1) FA, (2) SCF and LMO momentum distributions.

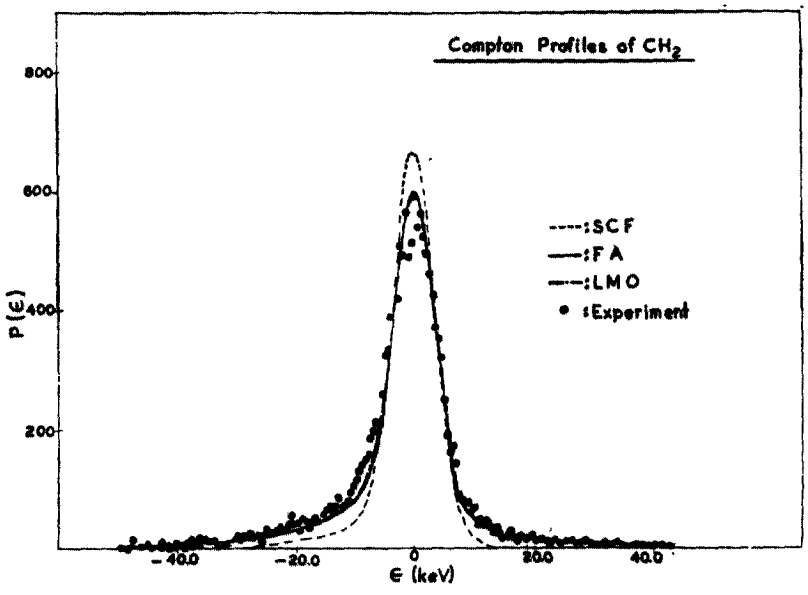

Fig. 3 Comparison of the calculated Compton profiles of CH_2 molecule with available experimental data.

mum both at electron velocity $v=0.005c$, where c is the velocity of light, while the LMO distribution is peaked at electron velocity $v=0.0069c$. The shapes of the tails at high momentum region are in close agreement between the FA and LMO distributions, in quite differing from the SCF distribution. This indicates that the FA and LMO approximations made on the position space wavefunctions for CH_2 molecule are internally consistent at high velocity region.

The Compton profiles calculated from those three momentum distributions are shown in Fig. 2. The peak portions of the profiles are contributed by the low momentum electrons while the tails of the profiles are provided by the high momentum electrons. As shown in Fig. 2 we also have differences in shape, height, and width of the Compton profiles because of the contribution from different shape of the momentum distributions.

It could be interesting to see how the approximations made on the motion of the electrons in CH_2 molecule bring those theoretical Compton profiles into the experimental profile. The experimental Compton profile of CH_2 molecule is available[7] but it was influenced by the energy broadening due to the resolution of experimental apparatus. Thus, the available measured spectrum was actually the fold of the broadening of the electron motion and the broadening of the instrumental effects in experiments. The resolution of the experimental apparatus was found to be Gaussian distribution of FWHM 5 keV. We now need to fold this 5 keV resoltution into the calculated Compton profiles to produce curves that can be compared directly to the experimental profile.

Fig. 3 shows the folded theoretical Compton profiles with the available experimental data. Comparison of the theoretical profiles with the experimental data indicates that they are in close agreement in the region from $\epsilon=2.5$ keV to $\epsilon=6.0$ keV. In the region of high momentum tails, however, the calculated profiles are somewhat narrower than the observed one, but the deviations are comparable to experimental errors, except the ones calculated from the SCF approximation, which contain significantly lower profiles

than the experimental one. It was seen in Fig. 3 that there is a symmetric deviation between the theory and the experiment. This deviation might come from the fact that the binding energy effect was entirely neglected in this calculation. Thus, it can be stated that the FA and LMO approximations give a better description about the motion of the high and intermediate momentum electrons in CH_2 than the SCF approximation. The SCF methods probably underestimated the kinetic energy of the inner shell electrons, and hence the momentum and the width of the Compton profile of the high momentum region.

The top portion of the profile is particularly sensitive to the low momentum electrons. The velocities are low and hence give the least broadening to the profile peak. They contribute, therefore, to the top of the peak. However, the detailed shape of tip of peak in the experimental profile was already masked out by the 5 keV instrumental resolution. Comparisons between the theoretical profiles and the experimental one are, therefore, difficult to make.

It can reasonably be concluded that the FA and LMO approximations can be used to provide a powerful tool for explaining and predicting momentum distributions and Compton profiles of molecules for which accurate wavefunction calculations are unfeasible.

We may refer briefly to other related matters. One of the great beauties of organic chemistry is the existance of groups of structurally similar molecules which chemists categorize as homologous series. The LMO approach, which agrees best with the observed results, might become extremely pewerful when applied to these series. Each series involves only a small number of different LMO types. Therefore, determination of a few LMO distributions and profiles will enable us to calculate these quantities for an entire series. By adding the LMO's for several functional groups to our set of C inner shell, C-H, and C-C bonds, we can derive momentum distributions and Compton profiles for nearly all commonly occuring organic compounds. Distributions and profiles for other homologous series or for molecules containing several functional groups can be easily derived by the same method.

References

1. Sang Kyun Nha, J. Korean Phys. Soc. (to be published)
2. Coulson and Duncanson, Proc. Camb. Phil. Soc. **38**, 100 (1942)
3. Sen'ich Togawa, Osmo Intrinen and Seppo Manninen, J. Phys. Soc. Japan **30**, 1132 (1971)
4. F. Herman and S. Skillman, "Atomic Structure Calculation", Prentice-Hall, Englewood Cliffs, N. J. (1963)
5. Morris Krauss, J. Res. Nat. Bur. Stand, **68A**, 635 (1964)
6. Irving R. Epstein, J. Chem. Phys. **53**, 4425 (1970)
7. S. K. Nha and J. A. McIntyre, Am. J. Phys. **40**, 1618 (1972).